



Deformation Characteristics of Ultra-Deep Foundation Pit in Yangtze River Floodplain with Multi-grade Dewatering

Tao Yang¹ · Liyuan Tong¹ · Hongbo Che¹ · Xin Yan¹ · Dan Li²

Received: 20 July 2021 / Accepted: 20 December 2021 / Published online: 25 January 2022
© Shiraz University 2022

Abstract

Multi-grade dewatering is an effective means to reduce the influence of large head difference on the foundation pit retaining structure and surrounding structures. The behavior of the waterproof curtain and the ground surface for the ultra-deep excavation and multi-grade dewatering in the Yangtze River floodplain was carried out through the case study. Then according to the field observation in terms of the data size, the position of maximum data, and the trend of data over time, a two-dimensional fluid–solid coupling calculation model considering transient dewatering was established to study the mechanism of multi-grade dewatering. The results show that the maximum horizontal displacement of the first waterproof curtain of the ultra-deep foundation pit constructed by the top-down method is $0.1H$, where H is the excavation depth. The ground settlement reaches $0.5\delta_s$ at a distance of $2H$ behind the curtain, where δ_s is the maximum settlement. The horizontal displacement variation of the curtain and the ground settlement variation during the structure construction stage accounted for 2/3 of those during the excavation stage. The decrease in water head between two waterproof curtains can reduce the horizontal displacement of the first waterproof curtain by 14.05% and increase the horizontal displacement of the second waterproof curtain and the ground settlement by 12.88% and 22.89%, respectively, in this study.

Keywords Fluid–solid coupling · Ground settlement · Horizontal displacement · Multi-grade dewatering · Ultra-deep excavation

1 Introduction

With the rapid formation of urban underground transportation network in China, riverside underground projects in many cities have entered a significant developing period. Taking Nanjing as an example, over 100 metro stations and

numerous other underground projects are located in the Yangtze River floodplain area (Li et al., 2018). The stratum structure in this area is a typical dual structure. The upper part of the stratum is mainly composed of silty clays with weak water permeability and low mechanical strength; the lower part is mainly composed of fine sand and gravelly sand, with large soil thickness, good permeability and water richness (Tao et al., 2020; Guo et al., 2020). Dewatering in deep foundation pits is a very important issue for underground engineering construction in this area. Improper dewatering design will easily lead to the instability and damage of foundation pit supporting structure (Feng et al., 2005; Kaneda and Yamazaki, 2009; Zhang et al., 2014). In addition, the dewatering of foundation pit will lead to the change of surrounding soil displacement and stress field (Shen et al., 2017; Wu et al., 2020). To study the deformation of the supporting structure and surrounding soil caused by different excavation and dewatering schemes in the Yangtze River floodplain area, a fluid–solid coupling simulation analysis that can reflect the interaction between the seepage field and the stress field should be used (Wang et al., 2014).

✉ Liyuan Tong
101010519@seu.edu.cn

Tao Yang
yangtao_nxh@seu.edu.cn

Hongbo Che
563844239@qq.com

Xin Yan
164947441@qq.com

Dan Li
1059194957@qq.com

¹ School of Transportation, Southeast University, Nanjing 210000, China

² Nanjing Urban Public Project Construction Centre, Nanjing 210019, China

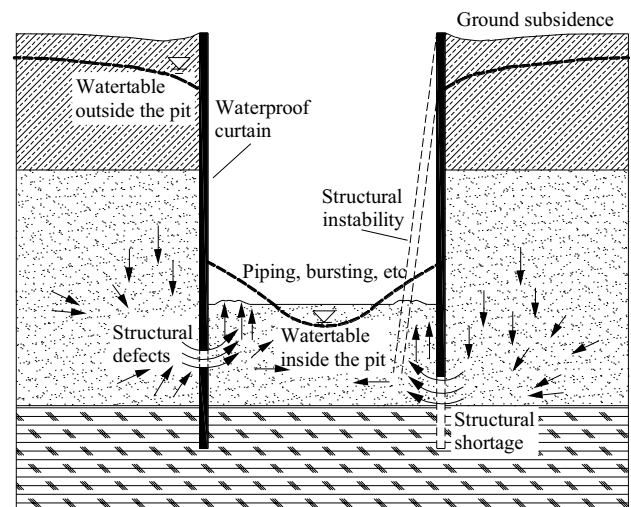
In recent years, many scholars in the field of geotechnical engineering studied the influence of foundation pit excavation and dewatering on surrounding areas (Zhou et al., 2010; Xu et al., 2014; Whittle et al., 2015; Tan and Lu, 2017; You et al., 2018; Wang et al., 2018; Zhang et al., 2018a, b; Zeng et al., 2019). Ou and Lai (1994) proposed an application of finite-element analysis using a combination of the hyperbolic and the Modified Cam-clay models, which were used to simulate the drained behavior of cohesionless soil and the undrained behavior of cohesive soil, respectively. Zheng and Zeng (2013) used three-dimensional fluid–solid coupling numerical analysis to simulate the field dewatering tests and then studied the mechanism of the horizontal displacement of the wall induced by dewatering of phreatic water before excavation. Bertoldo and Callisto (2016) studied the effect of the progressive dissipation of the excess pore-water pressures generated during the excavation stages through an advanced constitutive model, which was based on bounding surface plasticity and could consider the damage to the soil microstructure induced by plastic strains. Zhang et al. (2018a, b) presented details of the subsurface conditions, excavation support system, field instrumentation, and observed excavation responses, with a particular focus on the dewatering and associated ground settlement through a case in residual soil. Wu et al. (2019) presented an investigation on building settlement induced by dewatering for a deep excavation constructed in a deposit in Tianjin, China, where the geological conditions involved a multi-aquifer system with one phreatic aquifer over three confined aquifers.

However, previous studies pay little attention to the deformation characteristics of ultra-deep foundation pit in floodplain area and the mechanism of multi-grade dewatering in the process of ultra-deep excavation. To date, related engineering case reports are especially uncommon. Taking an ultra-deep foundation pit project in Yangtze River Floodplain as a case, this paper examined the role of the coupling of ultra-deep excavation and multi-grade dewatering on the waterproof curtain and the ground surface through adopting the fluid–solid coupling analysis method. This paper aims to propose suggestions of multi-grade dewatering according to the simulation and provide reference to similar engineering projects in Yangtze River Floodplain.

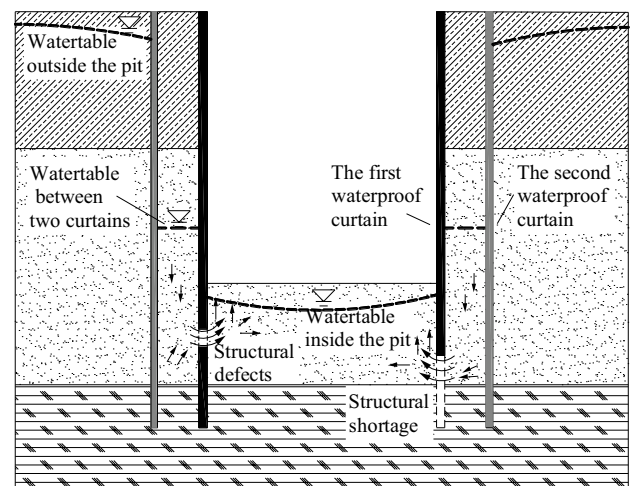
2 Design and Background of Multi-grade Dewatering

Multi-grade dewatering requires more than one waterproof curtain outside the foundation pit, and the first waterproof curtain also serves as the retaining wall. The form of the curtain can be diaphragm wall, bored piles, plain concrete wall, double row mixing piles and high pressure jet grouting piles, etc. In addition, a certain

number of dewatering wells need to be set up between the curtains, which can be used as needed to reduce the water head step by step, to reduce the pore-water pressure acting on the first waterproof curtain (retaining wall). The multi-curtains increase the seepage path, which can reduce the risk of foundation pit intruding and piping, and avoid destructive impact on surrounding important buildings. As shown in Fig. 1a, it is difficult to guarantee the construction quality of waterproof curtain in the ultra-deep range, which can increase the probability of structural defects and make the structure not reach the design depth. Meanwhile, because of the dewatering in the pit, the high water head difference will penetrate the



(a) Groundwater distribution under conventional dewatering



(b) Groundwater distribution under multi-grade dewatering

Fig. 1 Groundwater distribution under conventional dewatering and multi-grade dewatering: **a** Groundwater distribution under conventional dewatering, **b** Groundwater distribution under multi-grade dewatering

wall defects, holes and joints, and then causes engineering disasters such as leakage, intrushing, piping, structural instability and ground subsidence (see Table 1). Figure 1b presents multi-waterproof curtains are set outside the pit. With the excavation process of the foundation pit, the water head in the two curtains can be reasonably adjusted by combining the monitoring data, to reduce the possibility of a series of engineering disasters caused by the dewatering in the pit.

The stratum in the floodplain area of the Yangtze River is a typical dual structure, the substructure of the soil layer is thick, with good permeability and water richness. Therefore, the construction quality problems of the deep wall, the ultra-high water head difference inside and outside the pit and the large deformation of the wall are more prominent in this area, and the risk of leakage, intrushing and piping are greater. In conclusion, it is of great significance to carry out multi-grade dewatering design in this area and summarize the response of the waterproof curtain and ground caused by the coupling of excavation and multi-grade dewatering based on field observation and numerical simulation.

3 Establishment of Numerical Model

The finite difference numerical analysis software is suitable for doing a coupled fluid-flow and mechanical calculation if the grid is configured for fluid, and if the Biot modulus and permeability are set to appropriate value. By using this software, a fluid–solid coupling calculation model considering transient dewatering was established according to the case in this paper. The key parameters such as soil permeability coefficient and dewatering well pumping velocity were preliminarily determined according to the dewatering scheme and field pre-dewatering test, and the other model parameters were checked by using the observed horizontal displacement of waterproof curtain and ground settlement during excavation.

3.1 Overview of the Case

The foundation pit was located on the south-eastern bank of the Yangtze River as a shield receiving shaft, only 100 m away from the river (see Fig. 2). There was a three-storey underground tunnel which has been completed and opened to traffic adjacent to the pit. The excavation site was 50.3 m

Table 1 Some excavation accidents induced by groundwater (Zhang, 2018)

No	Project	Excavation depth	Incident	Cause
1	Jinmao tower	19 m	Piping	The confined water was not isolated, and piping occurred at the dewatering well when the excavation reached 17.5 m
2	North Square of Shanghai south railway station	12.5 m	Piping	The confined water was not isolated, and piping occurred when the excavation reached the bottom
3	Hangzhou Qianjiang Century city	18 m	Inrushing	The confined water was not isolated, and intrushing occurred at the original survey hole when the excavation reached 10 m
4	Liyang Road Station of Shanghai Metro	12 m	The uplift of the pit bottom	The confined water was not isolated and the pressure reducing well is not set, which led to the uplift of the pit bottom exceeding the warning value
5	A vertical shaft of Shanghai Huangpu River Pipeline	24.0 m	Inrushing	The confined water was not isolated, and intrushing occurred when the excavation reached the bottom
6	Hangzhou Raffles Plaza	24.2 m	Inrushing	The confined water was not isolated, and intrushing occurred at the original survey hole when the excavation reached 14 m
7	Suzhou Zhongrun Plaza	22.15 m	Piping	During the excavation of the fourth layer, piping appeared in the weak part between impervious layer and engineering pile
8	Fuxingmen Station of Wuhan Metro	24.8 m	Inrushing	The failure of freezing and solid near the weak part of supporting structure led to intrushing
9	A vertical shaft of Nanjing Metro Line 10	30.5	Piping	Because of the defects in the waterproof curtain, and piping occurred when the excavation reached the bottom
10	An underground complex in Nanjing	41.4 m	Inrushing	An abandoned pile lead the deep confined water into the excavation face when the excavation reached 16 m

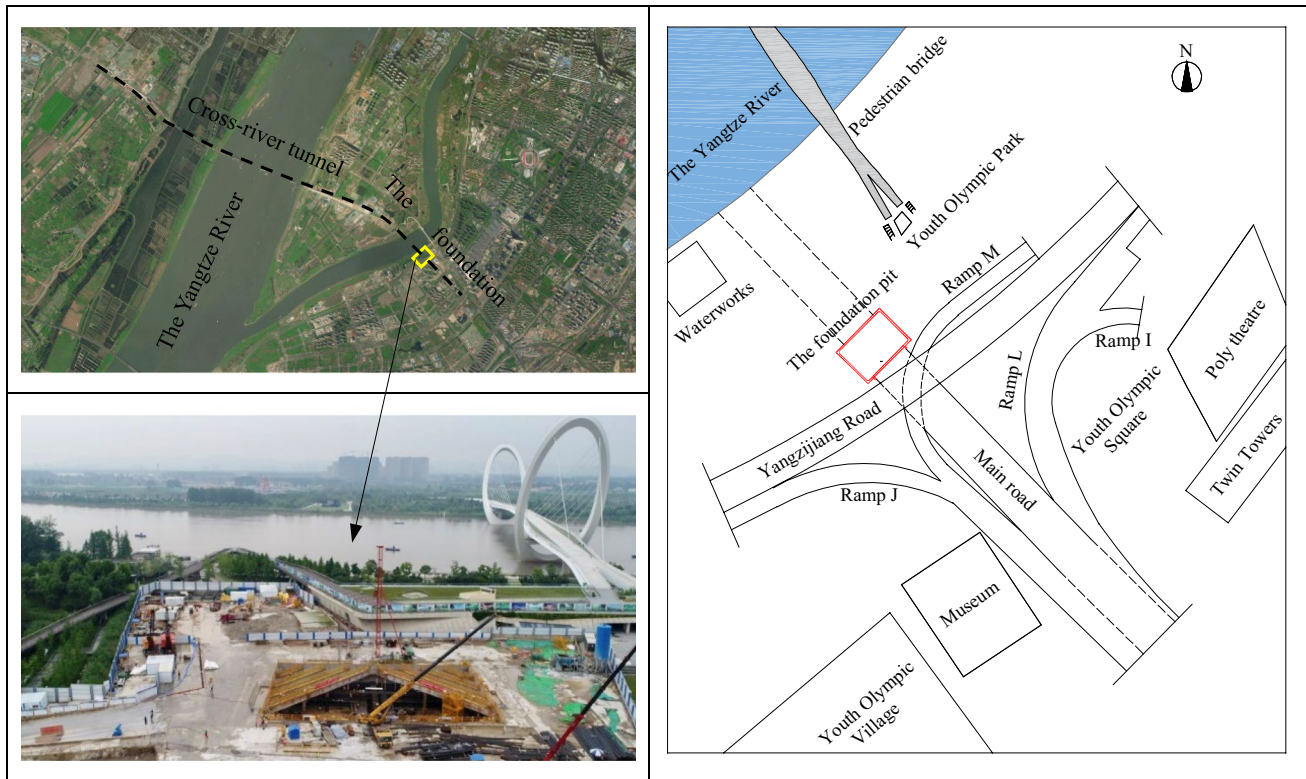


Fig. 2 Location and plane layout of the foundation pit

sides long with a width of 37.5 m, and the excavation depth was 38.9 m. The excavation was carried out with the top-down method and the first waterproof curtain (also as the retaining wall) formed a composite wall structure with the inner lining wall of the major structure to bear the force together. Four levels of slab braces and four levels of reinforced concrete braces formed the supporting structures of the pit (see Fig. 3). A 1200 mm thick diaphragm wall was used as the first waterproof curtain and installed as deep as 59.9 m. It entered into the moderately weathered sandy mudstone and was a "falling down" waterproof curtain. A 800 mm thick plain concrete wall was set as the second waterproof curtain at 2.5 m outside the first waterproof curtain, and the depth of the second waterproof curtain was the same as that of the first curtain.

According to the geotechnical investigation report, the soils on-site are Quaternary sediments. Due to long-term deposition by the Yangtze River, the upper stratum is mainly composed of silty clay, while the lower strata are mainly composed of fine sand and gravelly sand, forming the typical dual-structure stratum. The stratum distribution is shown in Fig. 3.

The on-site phreatic water was mainly distributed in layers of miscellaneous fill and silty clays with the water head of GL. -4.0 ~ -4.3 m. The confined water was mainly distributed in silty sand, fine sand, Medium-coarse sand and

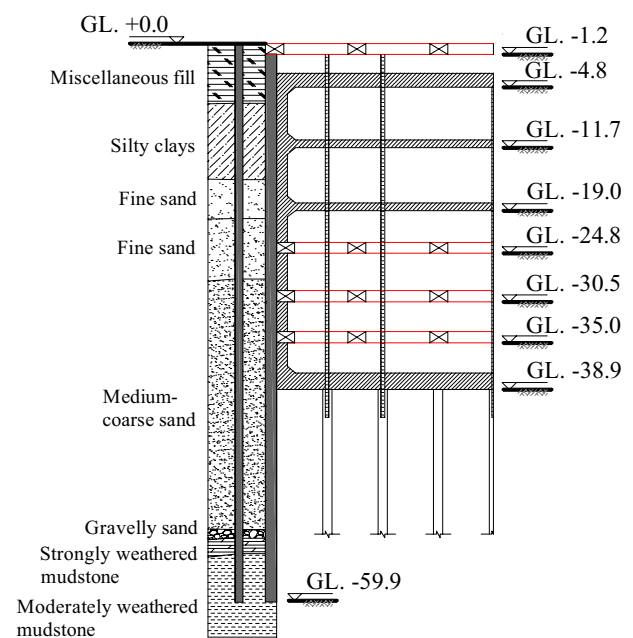


Fig. 3 Profile of the excavation and subsurface soil layers

gravelly sand with the water head of GL. -3.4 ~ -4.1. Ten dewatering wells were set in the pit, eight reserve dewatering wells were set between the two curtains, and twelve recharge

wells were arranged outside the pit. The layout of dewatering wells and recharge wells is shown in Fig. 4.

3.2 Model Constitutive and Parameters

This simulation used a plane strain model for analysis, and the size of the model was determined according to the influence range of excavation and the influence radius of dewatering. The influence radius of dewatering is estimated by the following empirical formula (Li et al., 2018):

$$R = 10s_w \sqrt{k} \tag{1}$$

in which s_w is the drawdown of water head (m); k is the weighted average value of permeability coefficient (m/d) of aquifer within the depth range of dewatering well. Taking the foundation pit as a dewatering well, through the calculation and analysis of the seepage analysis software MODFLOW, when the water head dropped to the bottom of the pit, the maximum drawdown of the water head outside the pit was 5 m, the weighted average value of the permeability coefficient of the aquifer within the depth range of the dewatering well was 3.58 m/d, and then, the influence radius of the dewatering was 179 m. The influence radius of foundation pit excavation unloading is generally 3~5 times of the excavation depth. Combining the above two influence radiuses, the horizontal direction of the model was 450 m. The vertical dimension is generally 3 times of the excavation depth, so the vertical direction of the model was 120 m. The water head along the right and left side were fixed, and the horizontal movements of nodes on the two sides were

restrained with the vertical movement allowed. The water head along the bottom was alterable, and the horizontal and vertical movement of all nodes at the bottom were fixed. According to the practical position of the filter tube to set the flow unit in the model and adopting the practical dewatering time to perform the fluid–solid coupling calculation.

The modified Cam-Clay model and Mohr Coulomb model were used to simulate cohesive soil and sandy soil, respectively. The original soil properties at the site were obtained from geotechnical investigation, empirical formula and laboratory tests, and the revised parameters are shown in Table 2.

In this analysis model, the liner elastic model was adopted for the waterproof curtain, the reinforced concrete braces and the lining wall. The elasticity modulus and the Poisson's ratio of the waterproof curtain were set to 32 GPa and 0.22. The elasticity modulus and the Poisson's ratio of the reinforced concrete braces and lining wall were 34 GPa and 0.22. The column pile was simulated by pile element with elastic modulus = 34.5 GPa and Poisson's ratio = 0.2. Because of the possible bending moment-induced cracking in concrete, the stiffness of the curtain and the liner wall were assumed to be 80% of the nominal value, whereas the axial stiffness for the reinforced concrete braces was 60% of the nominal value, considering bending which was caused by heaving of the column pile (Ou, 2006). Due to the possibility of water seepage at the joints of the curtain, a proper generalization assumption that the permeability coefficient of the curtain was set to 0.001 m/d was made for the waterproof curtain.

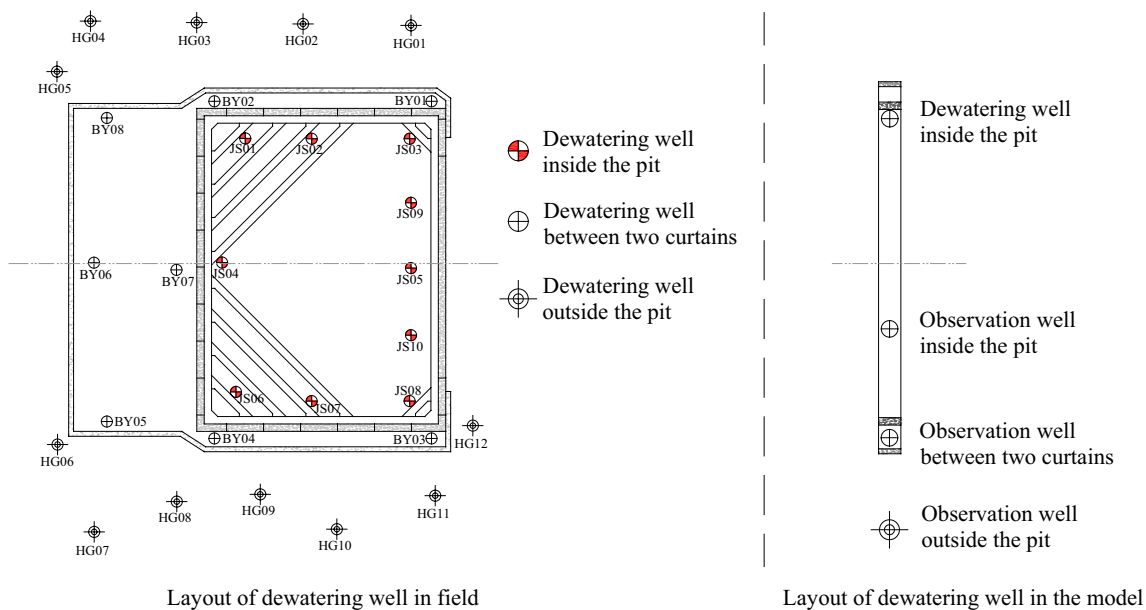


Fig. 4 Layout of dewatering well in field and model

Table 2 Physical and mechanical parameters of the soils

No	Soil layer	$\gamma/\text{kN}\cdot\text{m}^{-3}$	e	E_s/MPa	ν	c/kPa	$\varphi/^\circ$	$w/\%$	$K_H/\text{m}\cdot\text{d}^{-1}$	$K_V/\text{m}\cdot\text{d}^{-1}$	Parameters for MCC model			
											M	λ	k	N_r
1	Miscellaneous fill	19.3	0.870	4.60	0.3	10.0	9.5	32.6	0.001	0.001	0.45	0.0825	0.0064	2.07
2	Silty clays	18.4	0.974	3.95	0.33	16.8	5.9	33.2	0.001	0.001	1.06	0.0838	0.0065	2.00
3	Fine sand	19.6	0.715	14.69	0.27	6.8	29.8	24.9	20	6	–	–	–	–
4	Fine sand	19.5	0.721	13.84	0.26	5.8	29.5	24.8	20	6	–	–	–	–
5	Medium-coarse sand	19.5	0.695	13.78	0.26	5.7	29.9	22.9	25	12	–	–	–	–
6	Gravelly sand	20.7	0.579	13.78	0.26	25.5	23	20.6	25	12	–	–	–	–
7	Strongly weathered mudstone	22.1	1	44.65	0.35	–	–	15.7	0.001	0.001	–	–	–	–
8	Moderately weathered mudstone	23.4	1	376.45	0.32	–	–	10.3	0.001	0.001	–	–	–	–
9	Slightly weathered mudstone	23.3	1	890.50	0.30	–	–	7.6	0.001	0.001	–	–	–	–

γ =unit weigh; e =void ratio; E_s = compression modulus; ν =Poisson's ratio; c =cohesion; φ =internal friction angle; w =water content; K_H = horizontal permeability coefficients; K_V = vertical permeability coefficients; M =frictional constant; λ =slope of the normal consolidation line; k =slope of the elastic swelling line; N_r =Specific volume

Table 3 Design and results of field pre-dewatering test

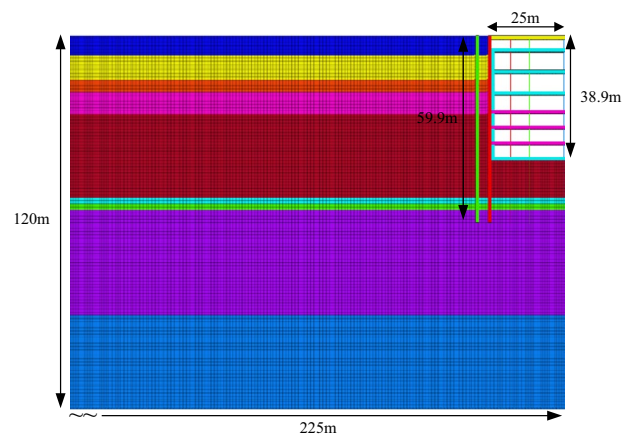
No		Dewater time/h	Number of wells	Single well pumping capacity/ $\text{m}^3\cdot\text{h}^{-1}$	Head drops in the pit/m	Head drops between the two curtain/m	Head drops outside the pit/m
1	Field test	72	1	20	7.3	0.06	0.03
	Simulation	72	1	0.5	7.6	0.08	0.04
2	Field test	162	6	15	16.7	0.16	0.11
	Simulation	162	1	2.25	17.2	0.20	0.14

3.3 Determination of Model Dewatering Parameters

In order to verify whether the water head in the pit could be controlled below the bottom, and whether the water-proof effect of the curtain could meet the requirements, this project conducted multiple sets of pre-dewatering tests before the excavation. In order to obtain the dewatering parameters required for the coupling calculation, two sets of field pre-dewatering test were selected for simulation comparison in this study. The layout of dewatering wells and observation wells in the model is shown in Fig. 4.

The first set of pre-dewatering test selected JS03 as dewatering wells, JS10, BY08 and HG07 as observation wells. The second set of pre-dewatering test selected JS01, JS02, JS03, JS04, JS05 and JS06 as dewatering wells, JS05, BY07 and HG07 as observation wells. The pumping velocity and time in the field and model are presented in Table 3 (Fig. 5).

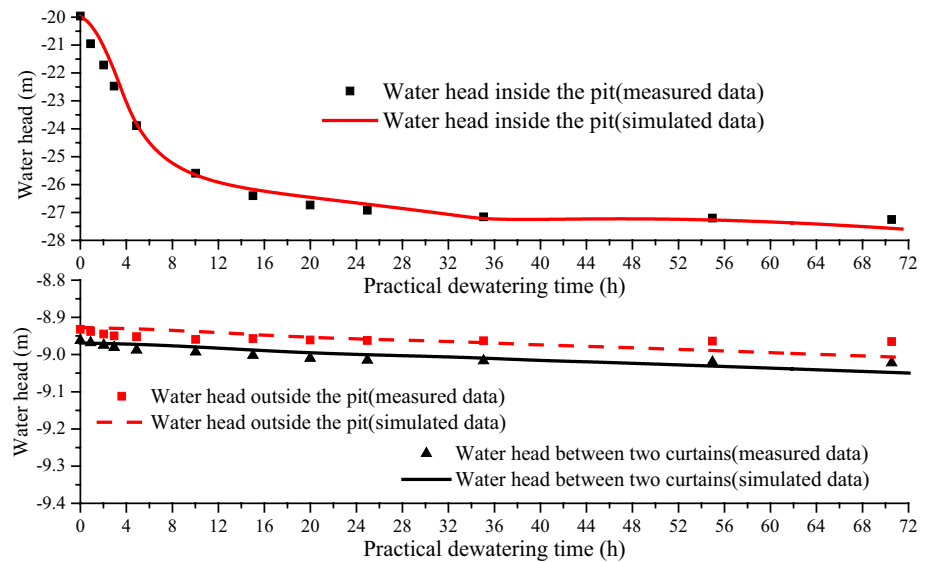
It can be seen from Fig. 6 that in the two sets of pre-dewatering test, the numerical simulation results were in reasonably agreement with the observed results. For the water head in the pit, the difference between the simulation value and the observed value was within 0.5 m. For the water head between the two curtains and the water head outside the pit,

**Fig. 5** Size and mesh of calculation model (half)

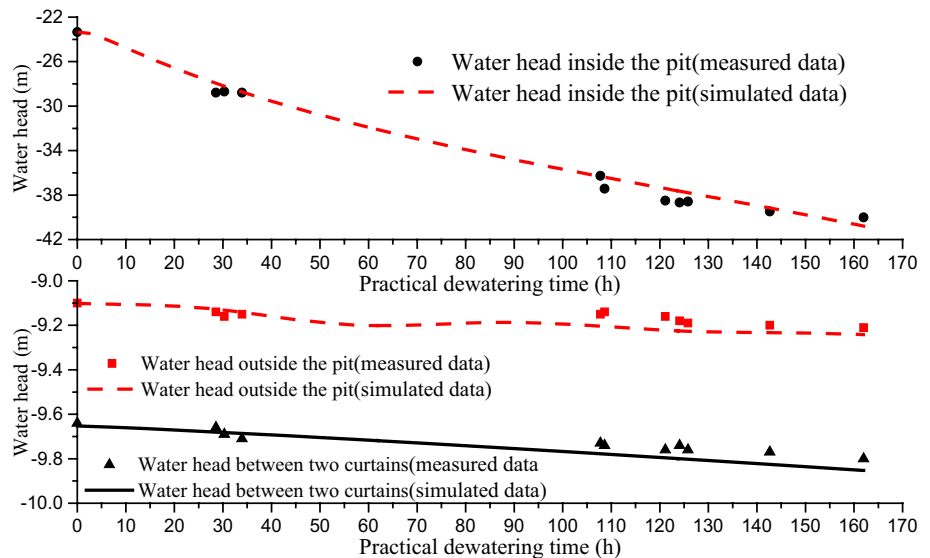
the difference between the simulation value and the observed value was within 0.05 m.

In conclusion, the model adopted in this study could adequately reflect the practical soil properties with respect to groundwater seepage. Therefore, it was justified that the model and the dewatering parameters could be used for subsequent simulation.

Fig. 6 Comparison between calculated values and monitoring values of pre-dewatering test: **a** The first set of pre-dewatering test, **b** The second set of pre-dewatering test



(a) The first set of pre-dewatering test



(b) The second set of pre-dewatering test

4 Analysis of Simulation and Observation Results

The project was constructed using the top-down method. The observed data showed that the horizontal displacement of the curtain and the ground settlement gradually increased over time, no matter during the excavation stage or the structure construction stage. In order to account for the influence of the excavation and dewatering on the surrounding area more accurately, the model needs to consider the time effect. So the complete fluid–solid coupling method was used to simulate the practical excavation and dewatering process. It should be noted that the dewatering

wells in the two walls were not opened during the practical excavation process because all the observed data were within the control indicators. Table 4 shows the schedule of the construction process.

This study adopted the observed data of the first waterproof curtain displacement and ground settlement on the north side of the foundation pit. In terms of data size, position of maximum data and development trend of data over time, the rationality of the model and simulation method used in this study was verified by comparison and analysis of different simulation methods and the deformation characteristics of ultra-deep foundation pit in floodplain area were also summarized.

Table 4 Construction stages

Step	Duration/d	Excavation depth/m	Construction activities
1	0–5	–	Pre-dewatering before excavation
2	5–15	4.8	Excavated to GL.–4.8 m
3	15–72	–	Top slab construction
4	72–82	6.9	Excavated to GL.–11.7 m
5	82–108	–	Second slab construction
6	108–118	7.3	Excavated to GL.–19.0 m
7	118–144	–	Third slab construction
8	144–152	5.8	Excavated to GL.–24.8 m
9	152–182	–	First reinforced concrete support construction
10	182–192	5.7	Excavated to GL.–30.5 m
11	192–210	–	Second reinforced concrete support construction
12	210–218	4.5	Excavated to GL.–35.0 m
13	218–248	–	Third reinforced concrete support construction
14	248–258	3.9	Excavated to GL.–38.9 m
15	258–299	–	Base slab construction

The water head should be 2 m lower than the bottom of the next layer before excavation of each layer

Figure 7 shows that the results of coupled simulation scheme adopted in this study had the highest matching degree with the observed data in the magnitude and position of the maximum horizontal displacement of the first

water-proof curtain. The results of the simulation scheme only considering excavation were the smallest, and the results of uncoupled simulation scheme were the largest. In addition, the horizontal displacement of the curtain can

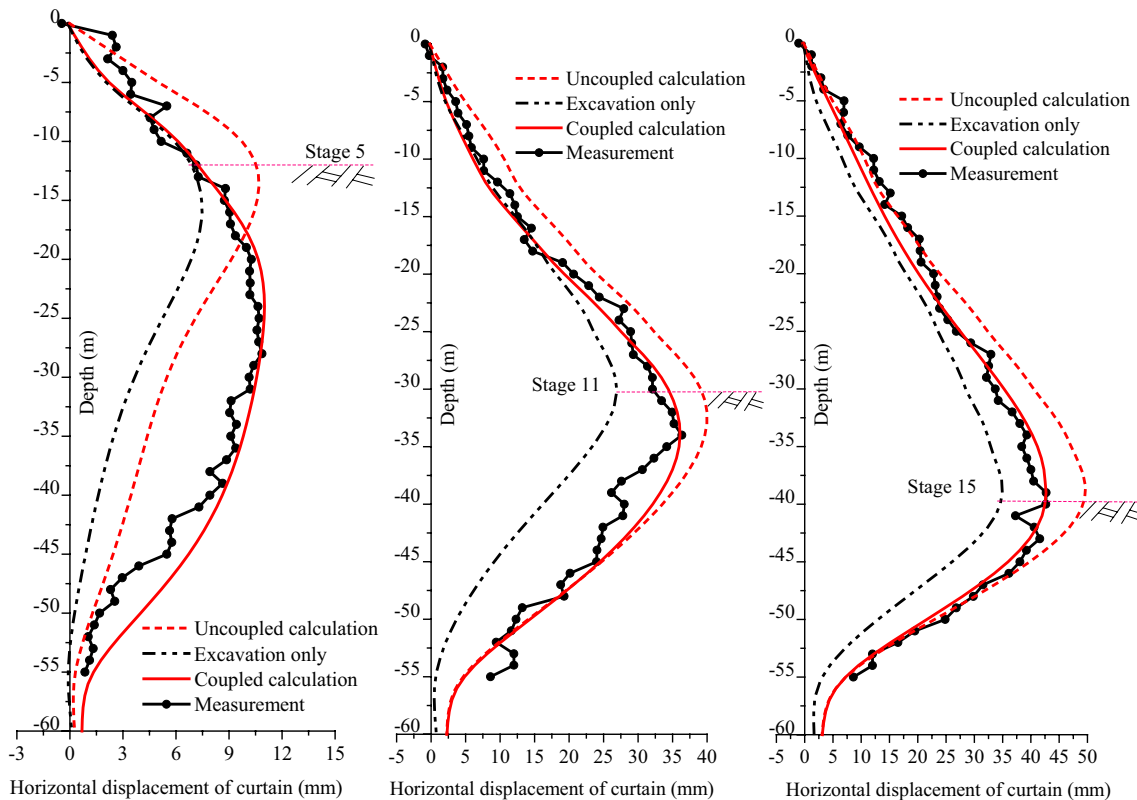


Fig. 7 Comparison of horizontal displacement of the first waterproof curtain

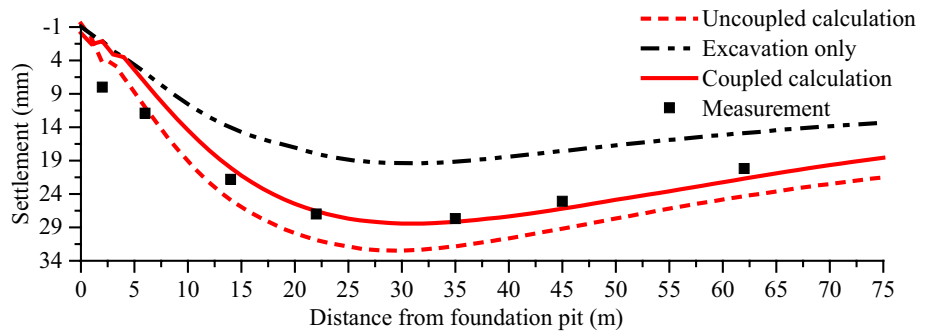
be controlled at about 0.1% of the excavation depth for the ultra-deep foundation pit constructed by the top-down excavation method, and the ratio was less than the other foundation pit constructed by the bottom-up excavation method in Yangtze River floodplain (Li et al., 2018).

Figure 8 shows that the results of coupled simulation scheme adopted in this study had the highest matching degree with the observed data in the magnitude and position of the maximum ground settlement. In addition, it can be observed that the maximum ground settlement was basically within the excavation depth limit, and the ground settlement value at twice the excavation depth limit still reached 1/2 of the maximum settlement value. The influence range of

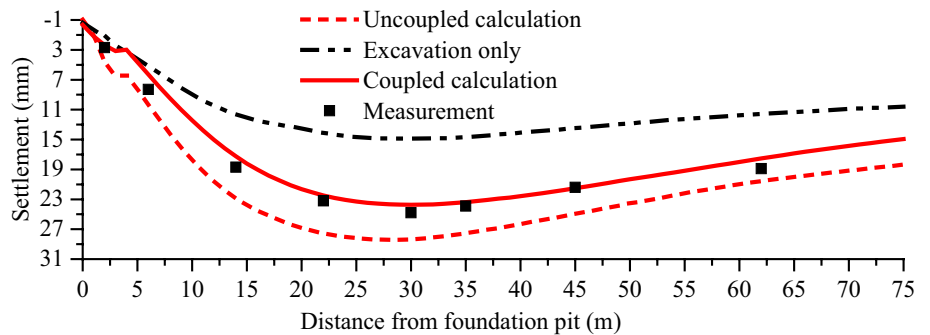
dewatering and excavation on ground settlement in the floodplain area is larger than that in Shanghai (Wang et al., 2011).

Figures 9 and 10 show that compared with uncoupled simulation, the coupled simulation method could better simulate the development trend of the horizontal displacement of the curtain and the maximum ground settlement over time. The coupled simulation could accurately reflect the increase in horizontal displacement of curtain and ground settlement during excavation stage and structure construction stage, while uncoupled simulation could not reflect the increment during the structure construction stage, and the increment during excavation stage was relatively large. In addition, according to the observed and simulated results,

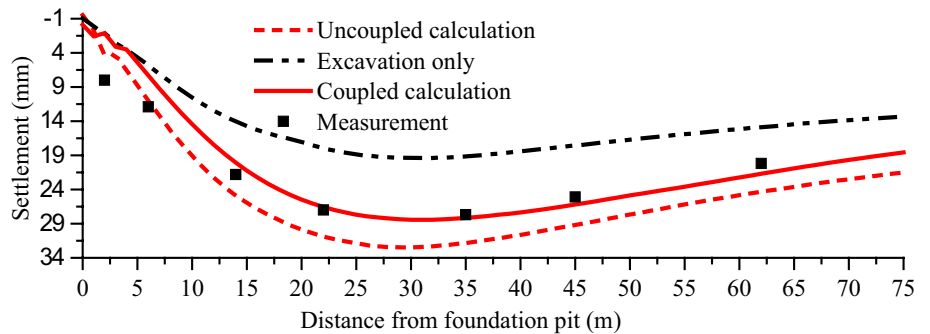
Fig. 8 Comparison of the ground settlement: **a** The ground settlement at stage 5, **b** The ground settlement at stage 11, **c** The ground settlement at stage 15



(a) The ground settlement at stage 5



(b) The ground settlement at stage 11



(c) The ground settlement at stage 15

the average value of deformation during the construction stage accounted for 2/3 of the average value of deformation during the excavation stage.

The uncoupled simulation method did not consider the influence of seepage, and the distribution of pore-water

pressure that changed with time was only obtained by dewatering. Figure 11 presents that the pore-water pressure around the curtain in the coupled simulation decreased significantly faster than that in the uncoupled simulation at different depths. This was because the soil around the curtain

Fig. 9 Variation of maximum horizontal displacement of the first curtain

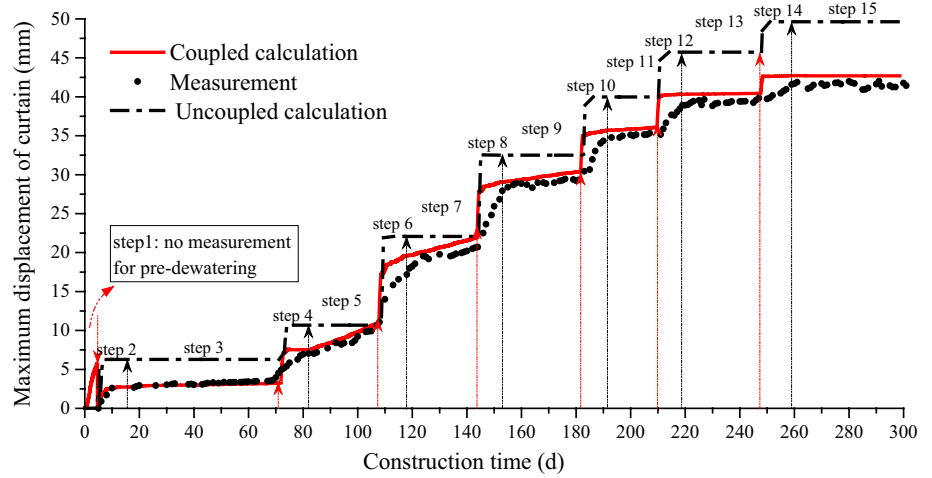


Fig. 10 Variation of maximum ground settlement

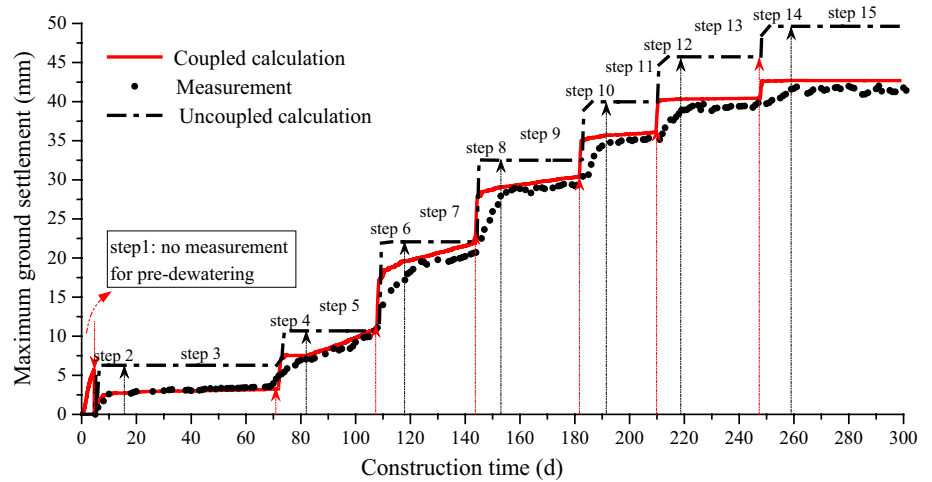
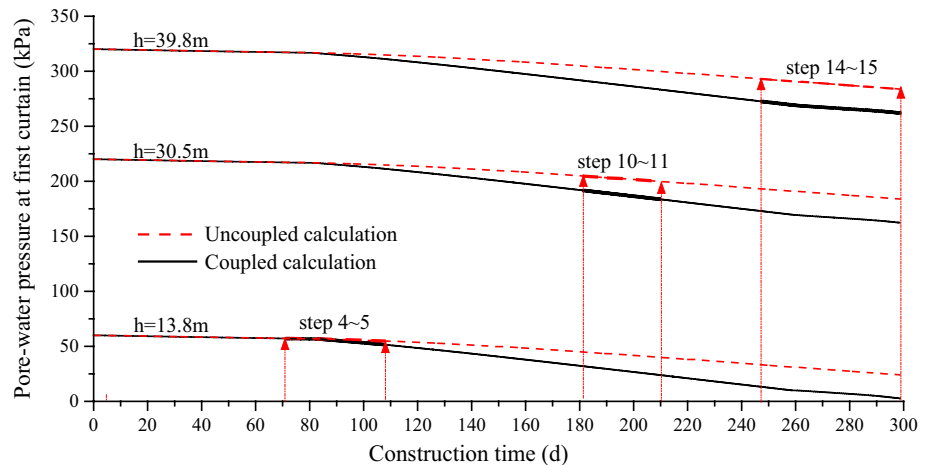


Fig. 11 Variation of pore-water pressure with construction process



had been consolidated to a certain extent with time in the coupled simulation scheme, the effective stress increased, the pore-water pressure decreased and then the soil strength increased. This explained the situation that the horizontal displacement of the curtain and ground settlement in the coupled simulation scheme were less than that in the uncoupled simulation scheme.

5 Study on the Effect of Multi-grade Dewatering

In order to examine the effect of multi-grade dewatering on the waterproof curtain and ground settlement, the following 7 working conditions considering the multi-grade water head were established as shown in Fig. 12 and Table 5. Based on the model verification and working condition design, the pore-water pressure and earth pressure distribution near the two curtains and the deformation laws of the two curtains and the ground settlement under the condition of excavation and multi-grade dewatering were studied.

5.1 Distribution of Pore-Water and Earth Pressure Near Two Curtains

Figures 13 and 14 show the distribution of pore-water and earth pressure near two curtains after the excavation of the foundation pit was completed. It can be seen that in the range of sandy soil, the pore-water pressure outside the first waterproof curtain increased linearly with the depth, while the earth pressure outside the first waterproof curtain did not increase linearly with the depth. The same law applied to the

distribution of pore-water and earth pressure near the second waterproof curtain. The primary reason was that the soil between the two curtains was in the deformation superposition area, the earth pressure near the first waterproof curtain belonged to the active earth pressure, and the earth pressure near the second waterproof curtain belonged to the passive earth pressure. In addition, due to the deformation of the two curtains at different depths was different, the influence of the two curtains on the soil was different at different depths. Therefore, in the fluid–solid coupling calculation of dewatering and excavation, the distribution law of pore-water and earth pressure was different along the depth.

It can also be seen from Figs. 13 and 14 that the variation of pore-water pressure corresponding to each depth under different working conditions was greater than the variation of earth pressure. For example, at the depth of 40 m of the first waterproof curtain, the pore-water pressure under practical working conditions was 252 kPa larger than that under the working condition with a head difference of 0 m, while the earth pressure decreased by 226 kPa. The situation was similar with the second waterproof curtain at the same depth. Therefore, as the head difference decreased, the total stress measured outside the first waterproof curtain and inside the second waterproof curtain decreased.

Figure 15 shows the variation of pore-water and earth pressure outside the first waterproof curtain at the depth of 39.8 m with the excavation process. It can be seen that under the practical working condition, the pore-water pressure decreased slowly due to the leakage of the curtains and other factors, and the earth pressure decreased rapidly during the excavation stage because of the horizontal displacement of the first waterproof curtain. During

Fig. 12 Multi-grade dewatering during excavation

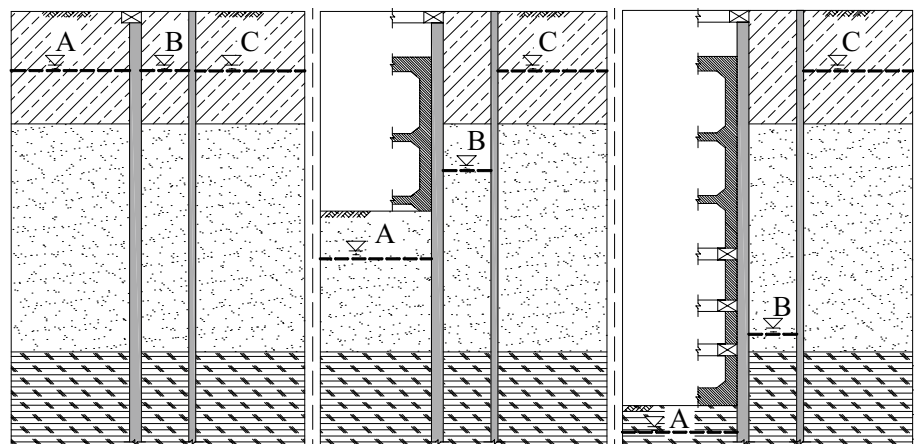
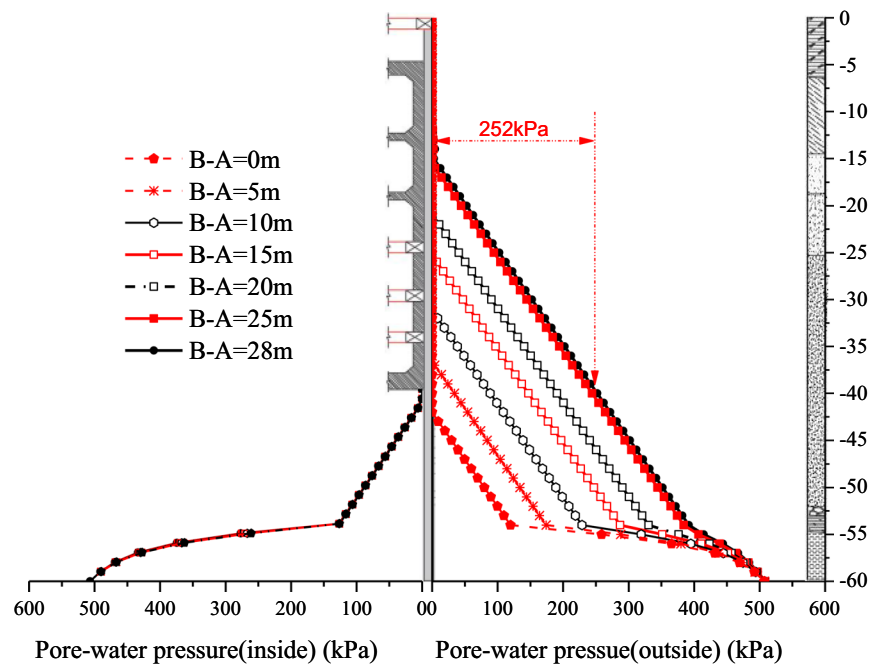


Table 5 Working condition design

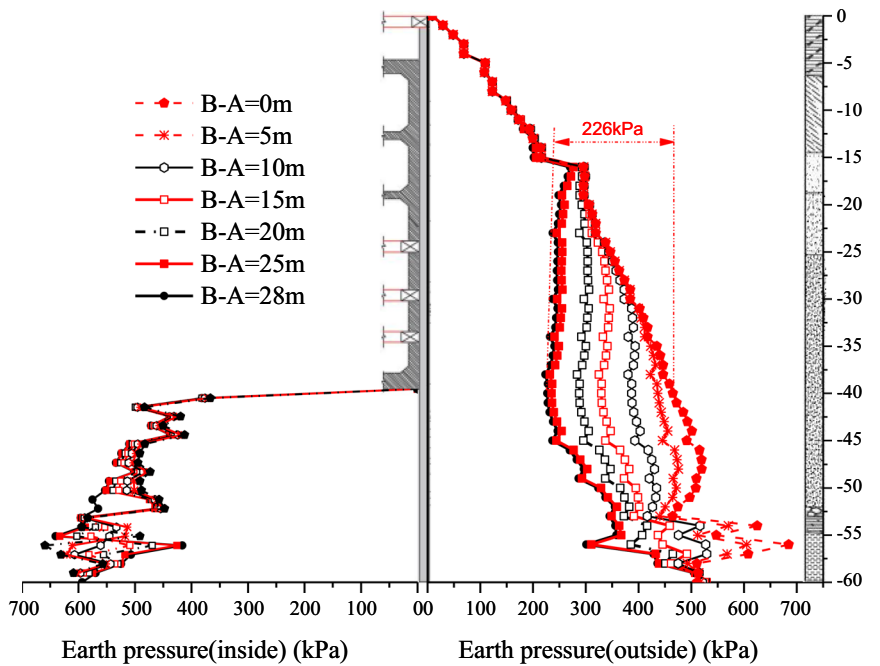
Working condition	1 (practical condition)	2	3	4	5	6	7
Head difference B-A (m)	28	25	20	15	10	5	0

The head difference B-A remains unchanged during the excavation, and no dewatering outside the pit

Fig. 13 Distribution of earth and pore-water pressure near the first waterproof curtain: **a** Distribution of pore-water pressure inside and outside the first waterproof curtain, **b** Distribution of earth pressure inside and outside the first waterproof curtain



(a) Distribution of pore-water pressure inside and outside the first waterproof curtain

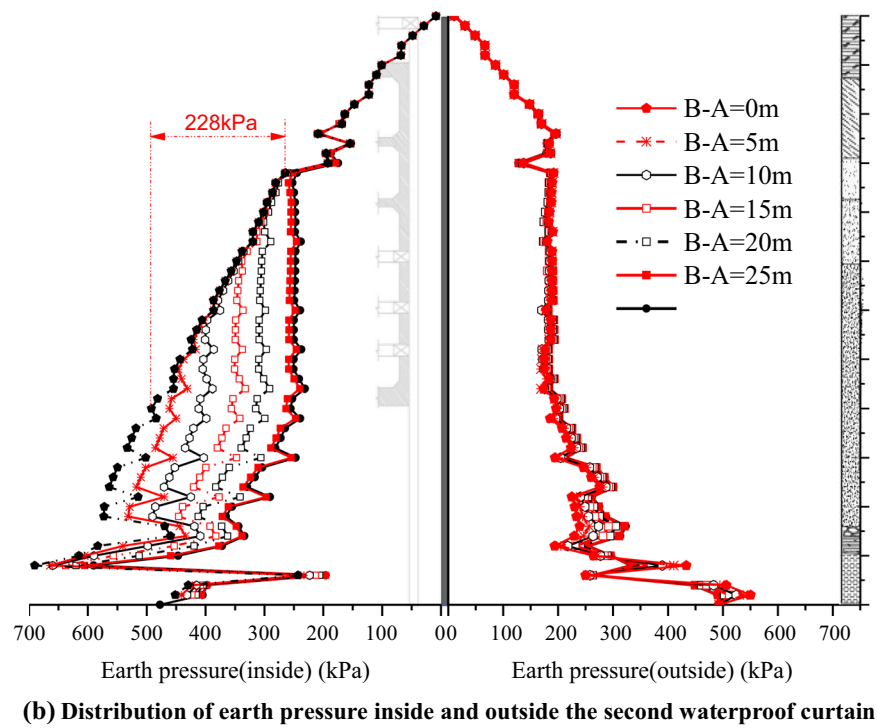
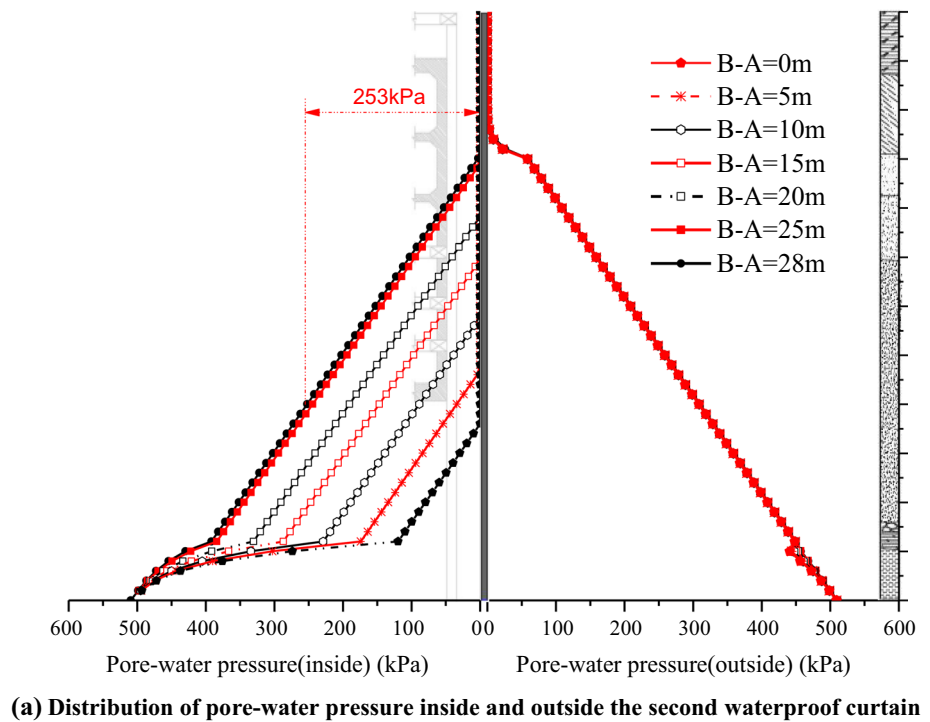


(b) Distribution of earth pressure inside and outside the first waterproof curtain

the construction stage of the foundation pit structure, the earth pressure increased slowly as the pore-water pressure decreased. Under the working condition of the head difference was 0 m, because of the continuous dewatering during the excavation process, the pore-water pressure outside the first waterproof curtain decreased gradually, resulting in the continuous increase in the earth pressure at the same

location. Meanwhile, it can be seen that the pore-water pressure in the two walls performs larger change than the earth pressure, which leading to the final total stress acting on the first waterproof curtain was lower than that in the practical working condition. The result also applied to the second waterproof curtain.

Fig. 14 Distribution of soil and pore-water pressure near the second waterproof curtain: **a** Distribution of pore-water pressure inside and outside the second waterproof curtain, **b** Distribution of earth pressure inside and outside the second waterproof curtain



5.2 Horizontal Displacement of Curtain and Ground Settlement

It can be seen from Figs. 16 and 17 that the larger the horizontal displacement of the first waterproof curtain was, the smaller the horizontal displacement of the second

waterproof curtain and ground settlement were. When the water head between the two curtains was equal to the water head in the foundation pit, the horizontal displacement of the first waterproof curtain was 36.7 mm, and the largest horizontal displacement of the second waterproof curtain and ground settlement were 44.7 mm and 34.9 mm,

Fig. 15 Variation of pore-water and total pressure outside the first waterproof curtain at the depth of 40 m: **a** Variation of pore-water pressure, **b** Variation of total pressure

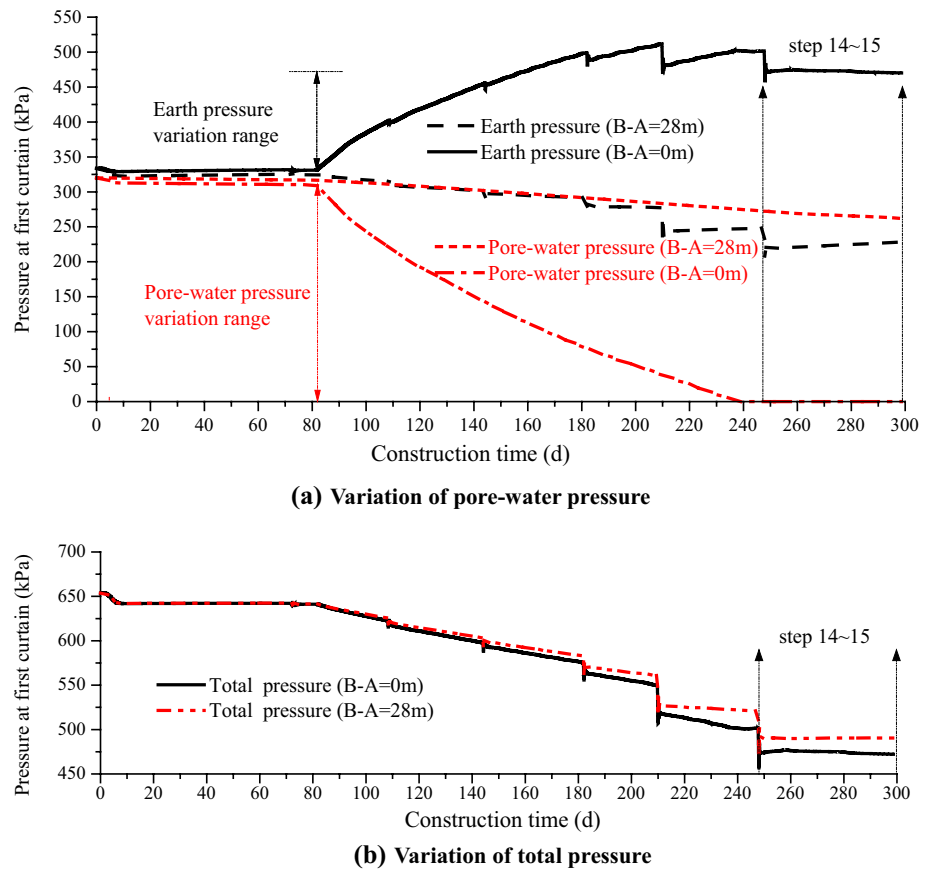
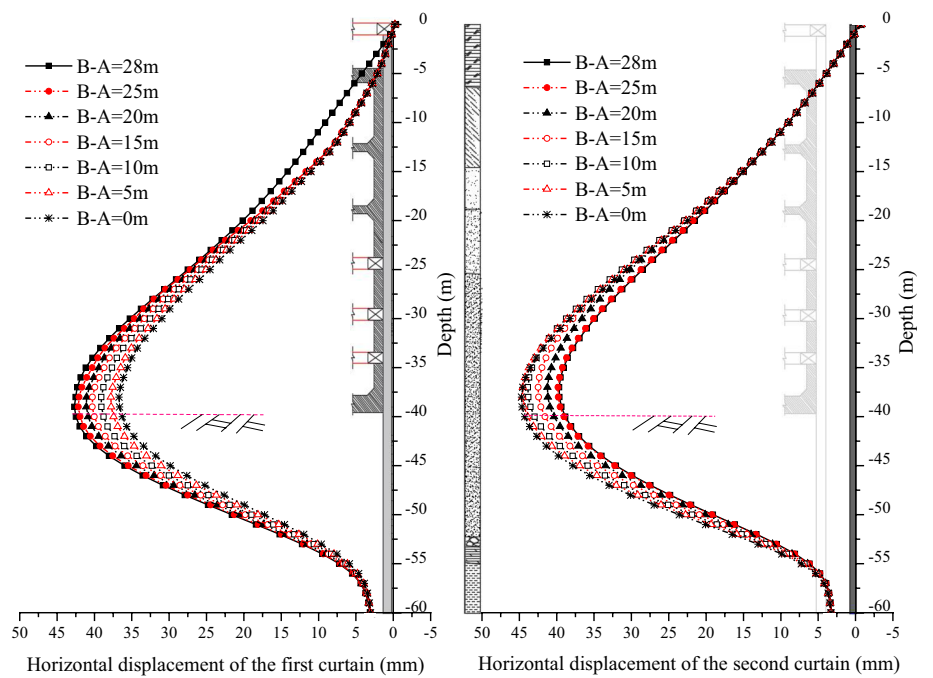


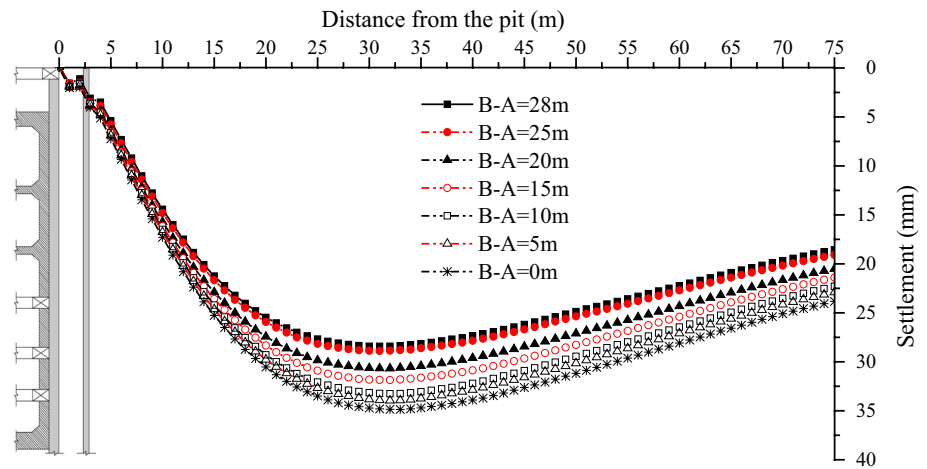
Fig. 16 The horizontal displacement of the first and second waterproof curtain



respectively. When the water head in the foundation pit was 28 m higher than the water head between the two curtains which is corresponding to the practical working conditions,

the horizontal displacement of the first waterproof curtain was 42.7 mm, and the horizontal displacement of the second waterproof curtain and the ground settlement were

Fig. 17 The ground settlement under different working condition



39.6 mm and 28.4 mm, respectively. With the decrease in the water head between the two curtains, the change rates of the first waterproof curtain deformation and the ground settlement could reach -14.05% and $+22.89\%$, respectively (see Table 6).

Through the above analysis, it can be seen that with the decrease in head difference $B-A$, the total stress acting on the outside surface of the first waterproof curtain and the inside surface of the second waterproof curtain decreased. Then, the total stress difference on both sides of the first waterproof curtain decreased, and the total stress difference on both sides of the second waterproof curtain increased. The stress distribution made the horizontal displacement of the first waterproof curtain reduced, but the horizontal displacement of the water stop wall and the ground settlement increased. Therefore, the water head difference should be reasonably controlled in the process of excavation and dewatering according to the deformation control requirements of foundation pit support and the surrounding structures in the practical project.

6 Conclusion

Combined with the field observation of ultra-deep foundation pit engineering, the reasonable calculation model was established, and the coupling method considering transient precipitation is selected for simulation. The deformation characteristics of ultra-deep foundation pit in Yangtze

River Floodplain and the influence of fluid–solid coupling effect of ultra-deep excavation and multi-grade dewatering on the horizontal displacement of waterproof curtain and ground settlement were summarized through the analysis of observed data and simulation results. The following conclusions can be drawn:

1. The coupled simulation method considering the transient dewatering can simulate the practical observed results more accurately in terms of the data size, the position of maximum data and the trend of data over time. For similar projects, the method in this study can be used as the pre-analysis to optimize the design and guide the construction.
2. In Yangtze River floodplain, the deep horizontal displacement of the waterproof curtain of the ultra-deep foundation pit constructed by the top-down method can be controlled within 0.1% of the excavation depth, the ground settlement at 2 times the excavation depth limit reaches $1/2$ of the maximum settlement, and the average deformation variation during the construction stage accounts for $2/3$ of those during the excavation stage.
3. Multi-grade dewatering had different effects on the waterproof curtain and ground settlement. The reduction of the water head between the two waterproof curtains could reduce the horizontal displacement of the first waterproof curtain by 14.05% , and increase the horizontal displacement of the second waterproof curtain and the ground settlement by 12.88% and 22.89% , respec-

Table 6 Results of different working conditions

Working condition		1	2	3	4	5	6	7	The rate of change
Maximum deformation value (mm)	The first curtain	42.7	42.1	41.1	40.3	39.1	37.8	36.7	-14.05%
	The second curtain	39.6	39.8	41.2	42.5	43.9	44.6	44.7	$+12.88\%$
	Ground settlement	28.4	28.9	30.7	31.9	33.3	34.0	34.9	$+22.89\%$

tively, in this study. To reduce the negative impact, the head difference should be adjusted according to the specific deformation control requirements of the foundation pit support and the surrounding structure.

Funding Majority of the work presented in this paper was funded by the National Natural Science Foundation for Surface Project of China (Grant Nos. 51878157 and 41572273) and the Jiangsu Natural Science Foundation (Grant No. BK20181282). These financial supports are gratefully acknowledged.

Declarations

Conflict of interest No potential conflict of interest was reported by the authors.

References

- Bertoldo F, Callisto L (2016) Effect of consolidation on the behaviour of excavations in fine-grained soils. *Proc Eng* 158:344–349. <https://doi.org/10.1016/j.proeng.2016.08.453>
- Feng XL, Xiong WL, Hu T, Shen JT (2005) Application of 3d coupling model of seepage and stress for simulating deep foundation pits dewatering. *Chin J Rock Mech Eng* 24(07):1196–1201. <https://doi.org/10.1007/s11769-005-0030-x>
- Guo SL, Yan CH, Yu LC, You Y (2020) Design of the supporting structures for large and unusually shaped foundation pit near the Yangtze River. *Adv Civil Eng* 2020:3831805. <https://doi.org/10.1155/2020/3831805>
- Kaneda K, Yamazaki H (2009) Soil-water coupled analysis of low land widespread subsidence due to dewatering. *Low Technol Int* 11(2):47–52
- Li FM, Chen GX, Liu XZ (2018) Deformation characteristics of suspended curtain deep foundation pit of metro lines. *Chin J Geotech Eng* 40(12):2182–2190
- Ou CY (2006) *Deep excavation theory and practice*. Taylor and Francis, Taipei
- Ou CY, Lai CH (1994) Finite-element analysis of deep excavation in layered sandy and clayey soil deposits. *Canad Geotech J* 31(2):204–214. <https://doi.org/10.1139/t94-026>
- Shen SL, Wu YX, Misra A (2017) Calculation of head difference at two sides of a cut-off barrier during excavation dewatering. *Comput Geotech* 91:192–202. <https://doi.org/10.1016/j.compgeo.2017.07.014>
- Tan Y, Lu Y (2017) Forensic diagnosis of a leaking accident during excavation. *J Perform Construct Facil* 31(5):04017061. [https://doi.org/10.1061/\(ASCE\)CF.1943-5509.0001058](https://doi.org/10.1061/(ASCE)CF.1943-5509.0001058)
- Tao YQ, Deng YM, Du Y, Xu Y, Leng ZC, Ma T, Wang YX (2020) Sources and enrichment of phosphorus in groundwater of the Central Yangtze River Basin. *Sci Total Environ* 737:139837. <https://doi.org/10.1016/j.scitotenv.2020.139837>
- Wang WD, Xu ZH, Wang JH (2011) Statistical analysis of characteristics of ground surface settlement caused by deep excavations in Shanghai soft soils. *Chin J Geotech Eng* 33(11):1659–1666. <https://doi.org/10.1097/RLU.0b013e3181f49ac7>
- Wang CB, Ding WQ, Chen ZG, Zhu L (2014) Research progress on seepage coupling theory of super-deep foundation pit engineering. *J Tongji Univ (nat Sci)* 42(02):238–245. <https://doi.org/10.3969/j.issn.0253-374x.2014.02.011>
- Wang JX, Deng YS, Ma RQ, Liu XT, Guo QF, Liu SL, Shao YL, Wu LB, Zhou J, Yang TL, Wang HM, Huang XL (2018) Model test on partial expansion in stratified subsidence during foundation pit dewatering. *J Hydrol* 557:489–508. <https://doi.org/10.1016/j.jhydrol.2017.12.046>
- Whittle AJ, Corral G, Jen LC, Rawnsley RP (2015) Prediction and performance of deep excavations for courthouse station, Boston. *J Geotech Geoenviron Eng* 141:040141234. [https://doi.org/10.1061/\(ASCE\)GT.1943-5606.0001246](https://doi.org/10.1061/(ASCE)GT.1943-5606.0001246)
- Wu YX, Lyu HM, Han J, Shen SL (2019) Dewatering-induced building settlement around a deep excavation in soft deposit in Tianjin, China. *J Geotech Geoenviron Eng* 145:050190035. [https://doi.org/10.1061/\(ASCE\)GT.1943-5606.0002045](https://doi.org/10.1061/(ASCE)GT.1943-5606.0002045)
- Wu YX, Shen SL, Lyn HM, Zhou A (2020) Analyses of leakage effect of waterproof curtain during excavation dewatering. *J Hydrol* 583:124582. <https://doi.org/10.1016/j.jhydrol.2020.124582>
- Xu YS, Shen SL, Ma L, Sun WJ, Yin ZY (2014) Evaluation of the blocking effect of retaining walls on groundwater seepage in aquifers with different insertion depths. *Eng Geol* 183:254–264. <https://doi.org/10.1016/j.enggeo.2014.08.023>
- You Y, Yan CH, Xu BT, Liu S, Che CH (2018) Optimization design and construction schemes for a deep foundation pit near the Yangtze River, China. *J Rock Mech Geotech Eng* 10(3):555–566
- Zeng CF, Zheng G, Xue XL, Mei GX (2019) Combined recharge: a method to prevent ground settlement induced by redevelopment of recharge wells. *J Hydrol* 568:1–11. <https://doi.org/10.1016/j.jhydrol.2018.10.051>
- Zhang YQ (2018) *Study on the characteristic and control of soil deformation induced by dewatering in confined aquifer during excavation*. Shanghai Jiao Tong University, Shanghai
- Zhang G, Zeng CF, Diao Y, Xue XL (2014) Test and numerical research on wall deflections induced by pre-excavation dewatering. *Comput Geotech* 62:244–256. <https://doi.org/10.1016/j.compgeo.2014.08.005>
- Zhang WG, Goh ATC, Goh KH, Chew OYS, Zhou D, Zhang RH (2018a) Performance of braced excavation in residual soil with groundwater drawdown. *Underground Space* 3(2):150–165. <https://doi.org/10.1016/j.undsp.2018.03.002>
- Zhang WG, Wang W, Zhou D, Zhang RH, Goh ATC, Hou ZJ (2018b) Influence of groundwater drawdown on excavation responses: a case history in Bukit Timah granitic residual soils. *J Rock Mech Geotech Eng* 10(5):856–864. <https://doi.org/10.1016/j.jrmge.2018.04.006>
- Zheng G, Zeng CF (2013) Lateral displacement of diaphragm wall by dewatering of phreatic water before excavation. *Chin J Geotech Eng* 35(12):2153–2163
- Zhou NQ, Vermeer PA, Lou RX, Tang YQ, Jiang SM (2010) Numerical simulation of deep foundation pit dewatering and optimization of controlling land subsidence. *Eng Geol* 114:251–260. <https://doi.org/10.1016/j.enggeo.2010.05.002>